

1 **Drought rapidly diminishes the large net CO<sub>2</sub> uptake in**  
2 **2011 over semi-arid Australia**

3 Xuanlong Ma<sup>a,\*</sup>, Alfredo Huete<sup>a</sup>, James Cleverly<sup>b</sup>, Derek Eamus<sup>b</sup>, Frédéric Chevallier<sup>c</sup>,  
4 Joanna Joiner<sup>d</sup>, Benjamin Poulter<sup>e</sup>, Yongguang Zhang<sup>f,g</sup>, Luis Guanter<sup>h</sup>, Wayne Meyer<sup>i</sup>,  
5 Zunyi Xie<sup>a</sup>, Guillermo Ponce-Campos<sup>j</sup>

6 <sup>a</sup> Climate Change Cluster, University of Technology Sydney, Broadway, New South Wales,  
7 2007 Australia

8 <sup>b</sup> School of Life Sciences, University of Technology Sydney, Broadway, New South Wales,  
9 2007 Australia

10 <sup>c</sup> Laboratoire des Sciences du Climat et de l'Environnement, CEA/CNRS/UVSQ,  
11 Gif-sur-Yvette, France

12 <sup>d</sup> NASA Goddard Space Flight Centre, Laboratory for Atmospheric Chemistry and  
13 Dynamics, Greenbelt, Maryland, 20771 United States

14 <sup>e</sup> Institute on Ecosystems and Department of Ecology, Montana State University, Bozeman,  
15 Montana, 59717 United States

16 <sup>f</sup> Jiangsu Provincial Key Laboratory of Geographic Information Science and Technology,  
17 International Institute for Earth System Sciences, Nanjing University, Nanjing, Jiangsu,  
18 210023 China

19 <sup>g</sup> Jiangsu Center for Collaborative Innovation in Geographical Information Resource  
20 Development and Application, Nanjing, Jiangsu, 210023 China

21 <sup>h</sup> Helmholtz Centre Potsdam, GFZ German Research Centre for Geosciences, Potsdam,  
22 14473 Germany

23 <sup>i</sup> Environment Institute, Ecology and Environment Science, University of Adelaide, South  
24 Australia, 5005 Australia

25 <sup>j</sup> USDA Agricultural Research Service, Southwest Watershed Research Centre, Tucson,  
26 Arizona, 85719 United States

27 \* Correspondence and requests for materials should be addressed to X.M. (email:  
28 xuanlong.ma@uts.edu.au).

29 **Abstract**

30 Each year, terrestrial ecosystems absorb more than a quarter of the anthropogenic carbon  
31 emissions, termed as land carbon sink. An exceptionally large land carbon sink anomaly was  
32 recorded in 2011, of which more than half was attributed to Australia. However, the  
33 persistence and spatially attribution of this carbon sink remain largely unknown. Here we  
34 conducted an observation-based study to characterize the Australian land carbon sink through  
35 the novel coupling of satellite retrievals of atmospheric CO<sub>2</sub> and photosynthesis and in-situ  
36 flux tower measures. We show the 2010-11 carbon sink was primarily ascribed to savannas  
37 and grasslands. When all biomes were normalized by rainfall, shrublands however, were  
38 most efficient in absorbing carbon. We found the 2010-11 net CO<sub>2</sub> uptake was highly  
39 transient with rapid dissipation through drought. The size of the 2010-11 carbon sink over  
40 Australia (0.97 Pg) was reduced to 0.48 Pg in 2011-12, and was nearly eliminated in 2012-13  
41 (0.08 Pg). We further report evidence of an earlier 2000-01 large net CO<sub>2</sub> uptake,  
42 demonstrating a repetitive nature of this land carbon sink. Given a significant increasing  
43 trend in extreme wet year precipitation over Australia, we suggest that carbon sink episodes  
44 will exert greater future impacts on global carbon cycle.

## 45 **Introduction**

46 Since the beginning of the industrial age, human activities (fossil fuel combustion, land use  
47 change, etc.) have driven the atmospheric CO<sub>2</sub> concentration from about 280 parts per million  
48 (ppm) in around 1780 to over 400 ppm in 2015<sup>1,2</sup>. The burning of fossil fuels and other  
49 human activities are currently adding more than 36 billion metric tons of CO<sub>2</sub> to the  
50 atmosphere each year<sup>3</sup>, producing an unprecedented build-up of this important  
51 greenhouse-forcing agent. Each year, terrestrial ecosystems sequester on average about a  
52 quarter of fossil fuel emissions and help mitigate global warming<sup>1-5</sup>. However, the nature,  
53 geographic distribution of land carbon sinks, and how their efficiencies change from year to  
54 year are not adequately understood, precluding an accurate prediction of their responses to  
55 future climate change and subsequent influences on climate through carbon cycle-climate  
56 feedbacks<sup>6,7</sup>. Recent evidence suggests that global semi-arid ecosystems provide an important  
57 contribution to the global land carbon sink and can dominate inter-annual variability and the  
58 trend of global terrestrial carbon cycle<sup>8,9</sup>.

59 Previous studies of the semi-arid carbon sink primarily relied on model outputs<sup>8,9</sup>. The results  
60 can be subject to uncertainties in input variables such as the assimilation of datasets that are  
61 sparse in many regions of the world, and may be further confounded by model assumptions,  
62 as suggested by a previous study finding that models can differ substantially in predicting  
63 inter-annual variability of the terrestrial carbon cycle<sup>10, 11</sup>. More importantly, these studies do  
64 not fully utilise ground measurements of carbon fluxes (e.g., from eddy-covariance flux  
65 towers). An observation-based study of the spatial attribution and temporal evolution of  
66 extreme wet-year driven carbon sinks over semi-arid regions has yet to be conducted to date.

67 Amplification of the hydrological cycle as a consequence of global warming is predicted to  
68 increase the frequency and severity of drought in the future<sup>12,13</sup>. These extreme drought

69 events, if coupled with warmer temperatures, are expected to profoundly affect ecosystem  
70 function and structure, further exerting major impacts on the global carbon cycle and  
71 feedbacks to alter the rate of climate change<sup>13-20</sup>. Globally, a reduction in terrestrial primary  
72 productivity from 2000 to 2009 has been recorded primarily due to drought impact, which  
73 weakened the terrestrial carbon sink<sup>17</sup>. Regionally, the 2003 European warm-drought caused  
74 broad-scale declines in ecosystem productivity, led to a reverse of 4 years of carbon uptake<sup>21</sup>.  
75 The 2000-2004 drought reduced regional carbon uptake over western North America  
76 substantially<sup>22</sup>, and also caused large-scale vegetation die-off<sup>23-25</sup>, further releasing carbon  
77 stocks from biomass back to the atmosphere.

78 Global semi-arid ecosystems are mostly dominated by grasslands, shrublands, and  
79 savannas<sup>26-28</sup>. A combination of high biomass turnover rates and their presence in  
80 water-limited environments renders semi-arid ecosystems particularly sensitive to drought  
81 and wet events<sup>28-32</sup>. A recent study using flux tower measurements over semi-arid grasslands  
82 in southwest United States identified a precipitation threshold that a semi-arid system could  
83 switch from a net sink or a net source of carbon from year to year<sup>32</sup>. Meanwhile, a common  
84 temporal and spatial sensitivity of gross CO<sub>2</sub> uptake to water-availability over a broad  
85 diversity of semi-arid ecosystems in North America has also been reported<sup>33</sup>, indicating that  
86 fast ecophysiological responses are useful for predicting semi-arid carbon sink/source  
87 dynamics under future climatic water availability<sup>34</sup>. Global semi-arid ecosystems are  
88 currently threatened by increasing aridity and enhanced warming<sup>35,36</sup>, posing concerns on  
89 their sustainable ability to absorb carbon, maintain biodiversity, and support human  
90 livelihood. A better knowledge of the intrinsic link between hydroclimatic variations and  
91 carbon sink-source dynamics over global semi-arid regions, especially those within the  
92 Southern Hemisphere which have dominated the recent global land carbon sink anomaly<sup>8,9</sup>, is  
93 thus urgently needed. To-date, questions such as which ecosystems contributed most to the

94 2011 land carbon sink anomaly and how they respond when subsequently subjected to  
95 drought, remain largely unanswered. Carbon sink allocation into labile or more stable carbon  
96 reservoirs and the factors that govern source-sink sensitivity in semi-arid regions must be  
97 understood for prediction of long-term global carbon cycle-climate feedbacks.

98 Here, we assess the spatial allocation and temporal evolution of the land carbon sink over  
99 Australia in response to early 21<sup>st</sup>-century hydroclimatic variations. Australia, the driest  
100 inhabited continent in the world, is dominated by savannas, grasslands, and shrublands  
101 (Supplementary Fig. S1). We focus on Australia not only because of its recent impact on the  
102 global carbon cycle<sup>8,9</sup>, but also because it experiences the largest climate variability among  
103 the continents (Supplementary Fig. S2), thus it is of interest to know how ecosystems behave  
104 under such extreme climate variability. Specifically, we want to determine: 1) the detailed  
105 spatial allocation of the large net CO<sub>2</sub> uptake and variations in intrinsic efficiency of using  
106 rainfall for taking up carbon during abnormally wet periods; 2) the persistence of the large  
107 semi-arid net CO<sub>2</sub> uptake throughout following dry period; and 3) the recurrence of  
108 Australia's large net CO<sub>2</sub> uptake in other wet years.

109 To answer these questions, we employed a multiple observation-based, interdisciplinary  
110 approach. To provide a "top-down" atmospheric view of the carbon dynamics, we used  
111 inverted net ecosystem carbon production (NEP) derived from satellite retrievals of CO<sub>2</sub>  
112 concentration from Japanese Greenhouse Gases Observing Satellite (GOSAT). We also used  
113 remote sensing of vegetation photosynthetic activity, including enhanced vegetation index  
114 (EVI) from the Moderate Resolution Imaging Spectroradiometer (MODIS) onboard NASA's  
115 Terra satellite and solar-induced chlorophyll fluorescence (SIF) from the Global Ozone  
116 Monitoring Experiment-2 (GOME-2) sensor onboard EUMETSAT's MetOp-A/B satellites.  
117 The EVI and SIF were used in a complementary manner, as SIF is emission-based and

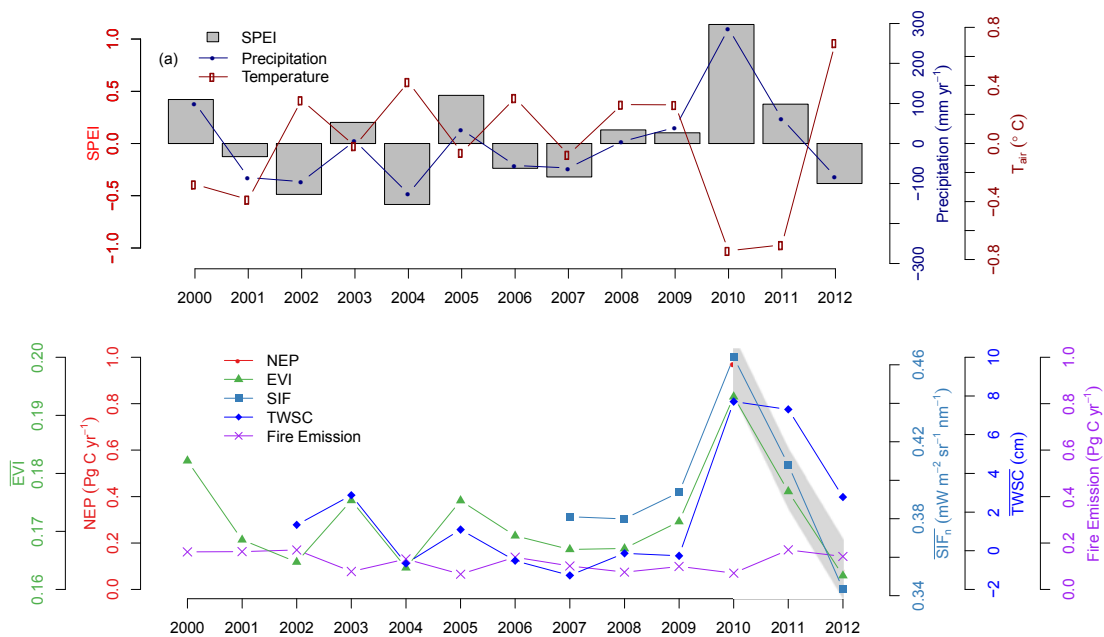
118 directly measures photosynthetic activity, while MODIS EVI is at a higher spatial resolution  
119 and enables the direct comparison with *in-situ* micrometeorological flux tower  
120 measurements. To characterize the hydroclimatic variations, we used the total water storage  
121 change (TWSC) from NASA's Gravity Recovery and Climate Experiment (GRACE)  
122 satellites and standardized precipitation-evapotranspiration drought index (SPEI) computed  
123 from long-term ground meteorological datasets. For SPEI, we used data computed at 6-month  
124 time scale considering the fact that vegetation across Australia primarily respond to drought  
125 at time-scales around 6-months or less. Lastly, as the most direct measure of  
126 ecosystem-atmosphere carbon exchange, we used NEP measured by *in-situ* eddy-covariance  
127 flux towers from two semi-arid ecosystems in Australia. Furthermore, to infer the  
128 contribution from fire emission to the semi-arid carbon-source dynamics, we employed the  
129 fire emission data from the fourth generation global fire emission database (GFED4.1s). A  
130 combination of multiple observation-based approaches will provide us the most direct and  
131 convergent evidence of the detailed spatial attribution, propensity, and the fate of the  
132 semi-arid carbon sink.

133 For our analyses, to accommodate the seasonal rainfall distribution over Australia, we used a  
134 'hydrological year' instead of using a calendar year. The hydrological year is defined as from  
135 September to next August based on mean monthly rainfall climatology, such that  
136 precipitation falling within a hydrological year was mainly used within that year for  
137 vegetation productivity. In following text, a hydrological year such as 2010-11 represents a  
138 12-months period from September-2010 to August-2011.

## 139 **Results and Discussion**

140 Early 21<sup>st</sup>-century hydroclimatic variations spanning Australia were characterised by below  
141 average precipitation coupled with anomalously high temperature (Fig. 1a). Annual

142 precipitation was below or near the historical average (1970-2013), while annual average  
 143 temperature was above or near the historical average throughout nearly the entire 2001-02 to  
 144 2008-09 (Fig. 1a). This warm-dry period was enclosed by two wet periods, 2000-01 and  
 145 2010-11, with another wet period occurring in 2005-06 (Fig. 1a). Australia's terrestrial  
 146 ecosystems were strong carbon sinks in 2010-11 hydrological year ( $\sim 0.97 \text{ Pg C yr}^{-1}$ ) (Fig. 1b;  
 147 Supplementary Table S1). This strong land carbon sink is corroborated by independent  
 148 observations from MODIS EVI and GOME-2 SIF, both showing a much enhanced  
 149 photosynthetic activity during the 2000-01, and 2010-11 wet episodes (Fig. 1b;  
 150 Supplementary Table S1). The magnitude of the 2010-11 enhanced land carbon sink as  
 151 derived from GOSAT inversion in this study, if reported based on calendar year, was  $0.77 \text{ Pg C}$   
 152 in 2011, which is very similar with  $0.79 \text{ Pg C}$  reported by Poulter *et al.*<sup>8</sup> or  $0.86 \text{ Pg C}$  from  
 153 another recent study<sup>37</sup>.



154

155 **Fig. 1. Inter-annual variation in climate, carbon flux and terrestrial primary productivity of Australia**  
 156 **from 2000-01 to 2012-13.** On the x-axis, 2000 represents the hydrological year starting from September-2000  
 157 to August-2011, and so on. (a) Variation in continental average annual Standardized  
 158 Precipitation-Evapotranspiration drought Index (SPEI), anomaly of annual precipitation ( $\text{mm yr}^{-1}$ ), anomaly of  
 159 annual mean daily temperature ( $T_{\text{air}}$ ,  $^{\circ}\text{C}$ ) over Australia from 2000-01 to 2012-13. Anomalies of precipitation  
 160 and temperature were computed with reference to the 1970-2013 base period. Positive SPEI indicates wetter



161 than the historical median; negative values, drier than median; (b) Variation in continental summation of Net  
162 Ecosystem Production (NEP) ( $\text{Pg C yr}^{-1}$ ), continental average of annual integrated Enhanced Vegetation Index  
163 (EVI), continental average of Solar-Induced chlorophyll Fluorescence ( $\text{SIF}_n$ , PAR normalized SIF,  $\text{mW m}^{-2} \text{sr}^{-1}$   
164  $\text{nm}^{-1}$ ), continental average of Total Water Storage Change (TWSC, cm), and continental total fire carbon  
165 emission ( $\text{Pg C yr}^{-1}$ ). NEP is derived from GOSAT atmospheric inversion modeling. The gray shaded area  
166 represents the Bayesian uncertainty range of inverted NEP ( $\pm 1\sigma$ ).

167 Consistent with the results from recent hydrological studies<sup>38,39</sup>, the large land carbon sink  
168 anomaly in 2010-11 corresponds with a large surplus of water storage (soil moisture + ground  
169 water) as indicated by GRACE TWSC (Fig. 1b). A sharp decline in both precipitation and  
170 GRACE TWSC after 2011, resulting in a dramatic reduction in NEP, EVI, and SIF from 2011  
171 to 2013 and demonstrating the systematic link between semi-arid carbon sink-source  
172 dynamics and hydroclimatic variations (Fig. 1b). This is consistent with a recent study using  
173 Australian land surface model, constrained by multiple observational data sources<sup>40</sup>, which  
174 also reported a similar sharp decline in continental NEP after the 2010-11 wet period<sup>41</sup>.

175 Meanwhile,  $\text{CO}_2$  emissions from fire burning were also enhanced following the 2010-11  
176 productive wet period (Fig. 1b). The total fire emission over Australia, as estimated by  
177 GFED4.1s, was 0.07 Pg C in 2010-11, ~42% below 2000-2013 average (Fig. 1b). The fire  
178 emission was boosted in 2011-12 (0.17 Pg C), one year followed the land carbon sink year,  
179 and was slightly reduced to 0.14 Pg C in 2012-13 (Fig. 1b; Supplementary Table S1). The  
180 total fire emission over Australia throughout the 2010-11 to 2012-13 period was 0.38 Pg C,  
181 about 25% of the size of total net carbon uptake (1.53 Pg C) over this period (Fig. 1b;  
182 Supplementary Table S1). This demonstrates the importance of fire emission as an important  
183 loss pathway over semi-arid ecosystems.

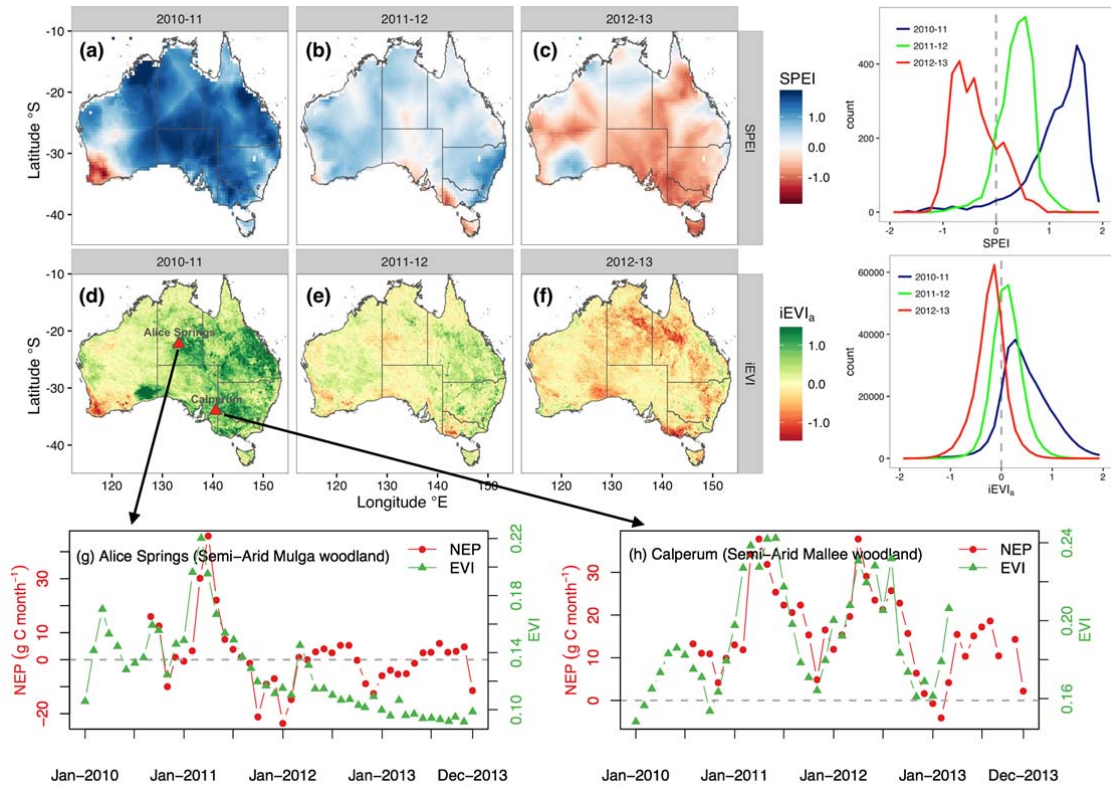
184 As a result of the combined effects from drought-induced reduction of photosynthetic activity  
185 and enhanced fire emissions, the percentage contribution of Australian terrestrial ecosystems  
186 to the global land carbon sink, as inferred from atmospheric inversion data, declined  
187 substantially from ~25% in 2010-11 to ~13% in 2011-12, and further reduced to ~2% in

188 2012-13. These observation-based results demonstrate that the rapid reversals of semi-arid  
189 carbon sink anomalies are important contributors to the inter-annual variability of the global  
190 terrestrial carbon cycle, as was shown through previous studies<sup>8,9,42</sup>.

191 Meanwhile, our results also indicate the potential ecological resilience of Australia's dryland  
192 ecosystems to altered hydroclimatic conditions, as they were able to sequester large amounts  
193 of carbon after protracted dry periods (Fig. 1). The resilience of Australian semi-arid  
194 ecosystems to drought may be attributed to the fact that these ecosystems are dominated by  
195 perennial, drought tolerant species such as *Acacia spp.* (mulga) and *Triodia spp.* (spinifex),  
196 each covers ca. 30-35% of Australian semi-arid land area<sup>43</sup>. These species can maintain  
197 foliage and minimal metabolic activity during the dry season or drought periods, largely  
198 attributed to their highly drought-adapted hydraulic architecture and their ability to tap deep  
199 soil water reserves with their lengthy root systems. Meanwhile, drought-adapted biota in  
200 these ecosystems also resulted in asymmetric response of Australia's dryland ecosystems to  
201 rainfall, in which these ecosystems responded more strongly to wet than to dry period<sup>44</sup>. As a  
202 result of above potential mechanisms, Australian semi-arid ecosystems were able to  
203 contribute to 2011 global land carbon sink anomaly significantly after the protracted early  
204 21<sup>st</sup>-century warm-dry period, further demonstrating the resilient nature of Australian  
205 semi-arid carbon sink (Fig. 1). Future studies are needed to look at the historical data in order  
206 to better understand the ecological resilience of Australia's dryland ecosystems in response to  
207 multiple drought and wet periods.

208 Carbon exchange over Australia is substantially affected by large-scale contrasting drought  
209 and wet conditions (Fig. 2). There was a transition from anomalously wet conditions in  
210 2010-11 (SPEI = 1.14) to anomalously dry condition in 2012-13 (SPEI = -0.38), especially  
211 over eastern Australia (Fig. 2a-c; Supplementary Fig. S3). At the same time, the positive

212 anomaly of MODIS EVI in 2011 switched to a negative anomaly in 2012, and by 2013, most  
 213 areas of Australia exhibited a strong negative MODIS EVI anomaly, suggesting a significant  
 214 reduction in terrestrial primary productivity and associated weakening of the strength of the  
 215 carbon sink under drought (Fig. 2d-f; Supplementary Fig. S3).



216

217 **Fig. 2. Biogeographic pattern of hydroclimatic condition and terrestrial primary productivity across**  
 218 **Australia from 2010-11 to 2012-13.** (a-c) maps of annual average SPEI; (d-f) maps of annual terrestrial  
 219 primary productivity anomaly (surrogated by anomaly of annual integrated EVI, or iEVI<sub>a</sub>); (g-h) MODIS EVI  
 220 alongside with *in-situ* eddy-covariance tower measured NEP at Alice Springs (semi-arid Mulga woodland)  
 221 and Calperum (semi-arid Mallee woodland) from Jan-2010 to Dec-2013. Right panels show frequency distribution  
 222 of SPEI and iEVI<sub>a</sub> for 2010-11 (blue), 2011-12 (green), and 2012-13 (red) using data from the all of Australia  
 223 respectively. Maps were drawn using R version 3.1.2 (<http://www.r-project.org/>).

224 As the most direct measurement of carbon exchange between an ecosystem and the  
 225 atmosphere, *in-situ* eddy-covariance (EC) flux tower measurements of NEP at two semi-arid  
 226 ecosystems were used as ground-truth to verify the patterns in the temporal evolution of  
 227 carbon fluxes as estimated from the "top-down" methods (Fig. 2g, h). At Alice Springs, the  
 228 ecosystem was a net sink of carbon in 2011, and rapidly switched to a weak carbon source in

229 subsequent 2012 and 2013 drought years<sup>43</sup> (Fig. 2g). At Calperum, each year from 2011 to  
230 2013 was a net sink of carbon, although the strength was weakened substantially in 2013 due  
231 to drought (Fig. 2h). Most importantly, we found strong agreement between *in-situ* EC flux  
232 tower measured NEP and MODIS EVI (Fig. 2g, h), suggesting that temporal variations in  
233 carbon fluxes at these semi-arid ecosystems were primarily driven by photosynthetic activity  
234 during the carbon sink period. This finding also supports the use of satellite measures of  
235 photosynthetic activity (MODIS EVI and GOME-2 SIF) for depicting the spatial allocation  
236 of the carbon sink over dryland ecosystems. Meanwhile, we also note the divergence between  
237 MODIS EVI and EC flux-tower NEP at Alice Springs during the carbon source period  
238 (2012-2013) (Fig. 2g), suggesting that remote sensing measures of photosynthesis is less  
239 suitable for identifying the location of carbon emissions during the source period, while more  
240 useful for inferring the location of carbon reservoirs during the sink period. The discrepancy  
241 between EVI and NEP during the dry period is likely due to: 1) EVI is a measure of  
242 photosynthetic capacity, which is more related to net primary productivity (NPP, the  
243 difference between photosynthesis and autotrophic respiration); 2) NEP is a balance between  
244 photosynthesis and ecosystem respiration. When NEP is primarily driven by variations in  
245 photosynthesis, it is expected to see a good correlation between NEP and EVI, as we saw  
246 during the land carbon sink year (Fig. 2g). When ecosystem is under drought stress and thus  
247 NEP is primarily driven by variations in ecosystem respiration, there should be a divergence  
248 between EVI and NEP, as during the period following the land carbon sink year (Fig. 2g).

249 We have shown that the NEP of carbon is primarily driven by photosynthesis during the  
250 carbon sink period over Australia's dryland ecosystems (Fig. 2g, h). We thus inferred the  
251 spatial location of the strength of net CO<sub>2</sub> uptake by partitioning anomaly of MODIS EVI  
252 into Australia's major biomes during the 2010-11 carbon sink period (Fig. 3). Among major  
253 biomes, savannas and grasslands had the highest rates of primary productivity anomaly

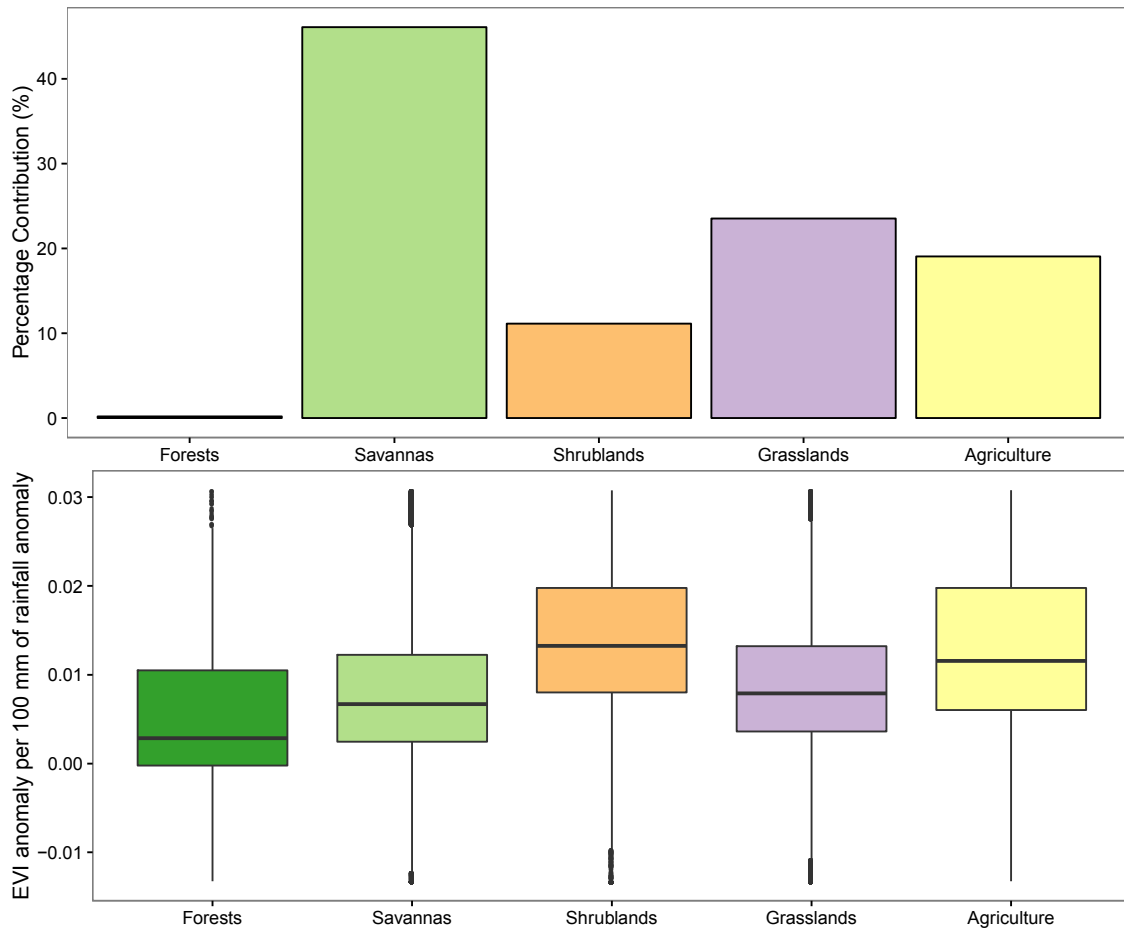
254 during the 2010-11 La Niña wet periods (Fig. 3a; Fig. 2d; Supplementary Fig. S1, Table S2).  
255 In 2010-11, about 46% of the terrestrial primary productivity anomaly was attributed to  
256 savannas and 24% to grasslands (Fig. 3a; Fig. 2d; Supplementary Fig. S1, Table S2),  
257 implying that these two biomes were potentially the biomes with the largest net CO<sub>2</sub> uptake  
258 in Australia during the carbon sink anomaly year, which is in line with another study based  
259 on model simulation<sup>45</sup>. The consistence between these independent studies increases the  
260 confidence of the spatial partition of the 2010-11 net CO<sub>2</sub> uptake into different biomes.

261 To further understand the variation in efficiency of using rainfall for taking up carbon during  
262 the 2010-11 carbon sink year, we calculated the ratio between MODIS EVI anomaly and  
263 rainfall anomaly for each pixel across Australia during the 2010-11 wet pulse. Our results  
264 showed that, despite the fact that savannas and grasslands are potentially the biomes with the  
265 largest net CO<sub>2</sub> uptake in 2010-11, shrublands, which are primarily located over central and  
266 southern Australia, have the highest efficiency in using rainfall anomaly for taking up carbon  
267 (Fig. 3b; Supplementary Fig. S4, Table S2). Our results indicated that mean  
268 rain-use-efficiency of shrublands is significantly higher ( $p < 0.0001$ , Student's *t*-Test) than  
269 that of grasslands, and also significantly higher ( $p < 0.0001$ ) than that of savannas.

270 Meanwhile, our results also highlighted the large within-biome variation in efficiency of  
271 using rainfall for generating productivity anomaly, as indicated by the fact that coefficient of  
272 variation (standard deviation / mean) ranges from 60% (shrublands) to 240% (forests)  
273 (Supplementary Fig. S4, Table S2). The much larger response of vegetation productivity to  
274 very wet year over drier shrublands than wetter biomes such as savannas and forests is likely  
275 due to the pulse-response behaviour of the drought-adapted plants in these ecosystems<sup>44</sup>.

276 Besides, we also noticed that for sparsely vegetated areas which have the largest positive  
277 asymmetric response of vegetation productivity to wet year<sup>44</sup>, our results showed that part of  
278 these sparsely vegetated ecosystems, primarily in Western Australia, did not exhibit a strong

279 productivity response in 2010-11 (Supplementary Fig. S4). The lack of response of these  
280 ecosystems to 2010-11 wet year may be attributed to the fact that a persistent decline in  
281 GRACE terrestrial water storage (TWS) trend has been observed over Western Australia  
282 since 2002<sup>39</sup>. This drying trend as indicated by GRACE TWS imply that vegetation over  
283 these regions were stressed during the 2002-2009 period and may have lost resilience, thus  
284 unable to respond strongly to the 2010-11 wet year. Future studies, with the incorporation of  
285 more field observations, are needed to investigate the exact mechanisms that explain the lack  
286 of response of ecosystems over Western Australia to the wet period. These patterns of varying  
287 rain-use-efficiency, as derived from observational datasets, are informative and reflect the  
288 differences in ecosystem-level carbon-water relationship. Therefore, Earth system models  
289 may consider using these patterns as observational test. Specifically, models may test their  
290 capability of simulating the spatial nature of the response of terrestrial carbon uptake per unit  
291 change in rainfall amount during the extreme wet years, i.e., the sensitivity of terrestrial  
292 carbon uptake to precipitation anomaly.

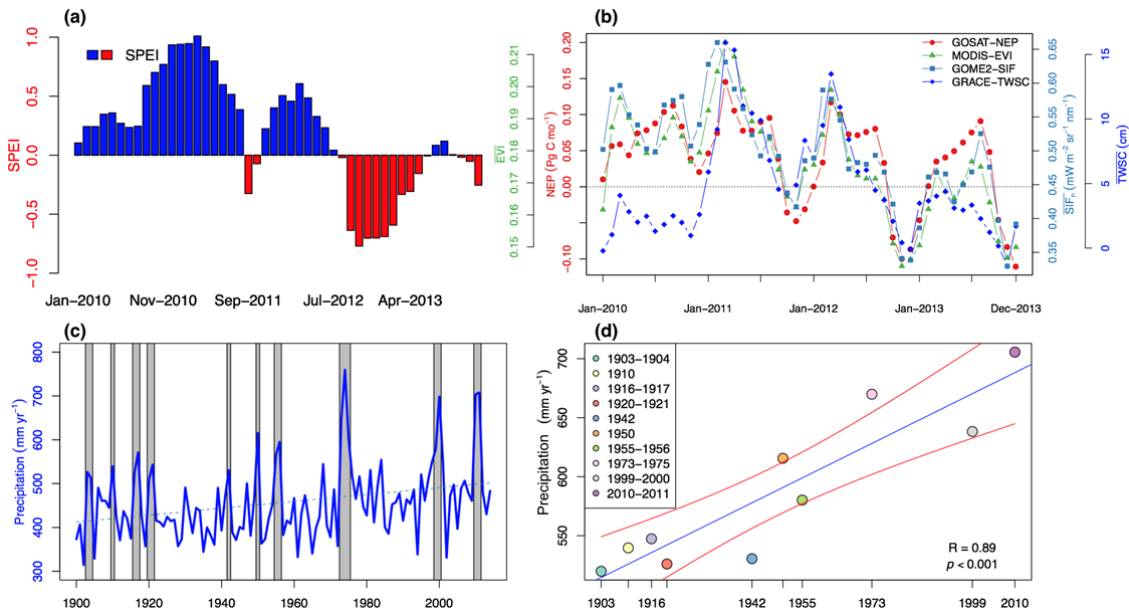


293

294 **Fig. 3. Partitioning of Australia's terrestrial primary productivity into contributions from major biomes**  
 295 **during the 2010-11 carbon sink period.** (a) Percentage contribution of each biome to Australian 2010-11  
 296 productivity anomaly (as indicated by anomaly of EVI). The percent contribution was calculated using MODIS  
 297 EVI. For each measure, the anomaly of EVI in 2010-11 hydrological year was calculated and then partitioned  
 298 spatially into different biome type; (b) box-plot of EVI anomaly in 2010-11 per 100 mm of rainfall anomaly in  
 299 2010-11 generated using all pixels within each biome. This is equivalent to the normalisation of EVI anomaly  
 300 for each biome by its total area and then further by rainfall anomaly. Thus the ratio is a measure of intrinsic  
 301 efficiency of an ecosystem in using rainfall for taking up carbon. The upper and lower hinges of the box-plot  
 302 correspond to the first and third quartiles (the 25th and 75th percentiles) of the data, while the upper and lower  
 303 whiskers correspond to the maximum and the minimum value of the data. The thick horizontal line within the  
 304 box represents the median value of the data.

305 We have shown that Australia's ecosystems are strong sinks of CO<sub>2</sub> during extreme wet  
 306 periods. An important question that remains is to what extent the strength of the wet  
 307 year-stimulated net CO<sub>2</sub> uptake is sustained through non-wet years? Throughout the entire  
 308 2010-11 wet period, Australia's ecosystems remained a large carbon sink, manifested by  
 309 enhanced photosynthetic activity marked by high MODIS EVI and GOME-2 SIF values (Fig.  
 310 4a, b). This active state continued into the first half of 2012 at a much lower rate, owing to

311 reduced water availability as indicated by both SPEI and GRACE TWSC (Fig. 4a, b;  
 312 Supplementary Fig. S5). Dry conditions prevailed from the late half of 2012 to 2013,  
 313 resulting in a significant reduction of the net CO<sub>2</sub> uptake from a strong net sink (-0.77 Pg C in  
 314 2010) to a weak sink (-0.12 Pg C in 2013), a 85% reduction in the strength of net CO<sub>2</sub> uptake  
 315 (Fig. 4a, b; Supplementary Fig. S5). Our multiple observation-based datasets thus  
 316 demonstrated the fact that the large semi-arid net CO<sub>2</sub> uptake originated from extreme La  
 317 Niña wet period to be very short-lived and a transitory event, in which drought occurrence  
 318 can rapidly reduce the magnitude of carbon uptake (Fig. 4a, b; Supplementary Fig. S5).



320 **Fig. 4. Reduction of net CO<sub>2</sub> uptake over Australia as determined by subsequent hydroclimatic**  
 321 **conditions.** (a) Monthly SPEI averaged across Australia from 2010 to 2013; (b) Variations of monthly NEP,  
 322 EVI, SIF, and TWSC aggregated across Australia from 2010 to 2013; (c) time series of average annual  
 323 precipitation across Australia from 1900 to 2013. Blue dashed line is the trend line, while grey vertical bars  
 324 indicate each very wet period since 1900; (d) trend in precipitation amount during the very wet periods (e.g.,  
 325 2010-11). Blue line is linear regression line and red lines indicate 95% confidence intervals. Before calculating  
 326 the precipitation amount during the very wet periods, the precipitation time series has been linearly detrended.

327 Australia is situated in a region of extreme climate variability, creating several-fold larger  
 328 fluctuations in precipitation and terrestrial primary productivity than encountered in all other  
 329 continents (Supplementary Fig. S2). Exceptionally large vegetation productivity was  
 330 recorded over Australia during both of the recent two La Niña-induced very wet periods



331 (2000-01 and 2010-11) (Fig. 1b), thus demonstrating that the large land carbon sink of  
332 Australia reported in 2010-11 was not an isolated and unique event, but rather a potentially  
333 episodic occurrence under strong wet phases. This is also reflected by the enhanced fire  
334 emissions throughout both the 2000-01 to 2002-03 and 2010-11 to 2012-13 periods (Fig. 1b).  
335 Precipitation and hence soil moisture availability are the primary drivers of semi-arid  
336 ecosystems carbon dynamics<sup>44</sup>; we therefore expect that the exceptionally large land carbon  
337 sink, coupled to very wet phases, will be observed again in the future.

338 An intriguing and important question is whether the magnitude of Australia's next carbon  
339 sink in a future wet episode will exhibit a similar strength as in 2010-11 or whether it will  
340 become stronger or weaker? The historical climatological record for Australia reveals that the  
341 precipitation amounts during wet years, such as 2000-01 and 2010-11, have increased  
342 significantly since 1900 (increasing by 11.66 mm per year,  $p < 0.05$ ) (Fig. 3c-d;  
343 Supplementary Fig. S6). Meanwhile, an overall wetting trend has resulted in the expansion of  
344 vegetation cover over Australia since 1981<sup>8,46</sup> (Fig. 4c; Supplementary Fig. S7). Recent study  
345 has found that dryland ecosystems in Australia tend to respond more strongly to wet period  
346 than drought, i.e., positive asymmetric type of responses, attributable to the pulse-response  
347 behaviour of these drought-adapted plants<sup>44</sup>. These findings together suggested that the  
348 magnitudes of the Australian semi-arid sink associated with wet-extremes will increase in  
349 coming decades. The consequence of this trend will have important implications for global  
350 carbon cycling, as shown during the 2011 global land carbon sink anomaly period<sup>8,9</sup>.

351 In summary, multiple independent lines of evidence create a compelling argument that  
352 extreme wet year driven, semi-arid land carbon sink events are transient and dissipate rapidly  
353 under ensuing drought. The efficiencies of these semi-arid carbon sinks are highly sensitive  
354 to hydroclimatic variations and are particularly vulnerable to drought. The spatial attribution

355 of the land carbon sink to tropical savannas and grasslands refines previous attributions to  
356 semi-arid ecosystems<sup>7,8</sup>. The finding of large variations in rainfall use efficiency among  
357 biomes for generating productivity anomaly in 2010-11 provides insight into the intrinsic  
358 effectiveness for taking up carbon. The two large carbon sink events, in 2000-01 and  
359 2010-11, were coupled with La Niña-induced wet pulses, and demonstrated an episodic  
360 nature of Australia's land carbon sink. Given a continuation of the increasing trend in extreme  
361 wet-year precipitation amounts since 1900 over Australia, we hereby suggest that the large  
362 land carbon sink will be observed again with greater magnitude in the future. We conclude  
363 that by contributing more positively to the global carbon balance with greater net CO<sub>2</sub> uptake  
364 during the forthcoming more intensive very wet years, Australia's ecosystems will play a  
365 more significant role in the global carbon cycle in coming decades. This study also  
366 demonstrated the great potential of integrating satellite and surface observations to provide a  
367 big, unifying picture of terrestrial carbon sink-source dynamics over a continental scale. The  
368 use of multiple observational data sources (e.g., GOSAT atmospheric CO<sub>2</sub> sampling,  
369 GOME-2 SIF, and GRACE TWSC) increases the robustness of land carbon sink-source  
370 analyses that will essentially lead to an improved understanding of the hydroclimatic drivers  
371 and pulse response behaviour of carbon fluxes over dryland ecosystems. The rapid  
372 dissipation of large semi-arid net CO<sub>2</sub> uptake under drought as revealed by this study presents  
373 important observational tests for Earth System models to accurately depict terrestrial carbon  
374 dynamics under intensified hydrological extremes.

## 375 **Methods**

376 We use multiple observation-based data sources to diagnose the geographic distribution and  
377 temporal evolution of Australia's land carbon sinks in extremely wet years. Continental-wide  
378 biospheric CO<sub>2</sub> fluxes were inverted using retrievals of atmospheric CO<sub>2</sub> from Japanese

379 Greenhouse gases Observing SATellite (GOSAT), with the Bayesian uncertainty statistics of  
380 the estimated fluxes were defined by a posterior error covariance matrix (see Supplementary  
381 information: Atmospheric inversion of biospheric carbon fluxes). Vegetation photosynthetic  
382 activity was indicated by two satellite measures: (1) Enhanced Vegetation Index (EVI), which  
383 is a composite measure of leaf area, chlorophyll content, and canopy architecture, derived  
384 from Moderate Resolution Imaging Spectroradiometer (MODIS) on-board NASA's Terra  
385 satellite (MOD13C1, Collection 5); (2) Solar-Induced chlorophyll-Fluorescence (SIF), which  
386 is emitted by the photosystem II of the chlorophyll molecules of assimilating leaves, derived  
387 from the Global Ozone Monitoring Experiment-2 (GOME-2) instrument on-board  
388 EUMETSAT's MetOp-A/B satellites (version 26, level-3) (see Supplementary information:  
389 Satellite measured vegetation photosynthetic capacity). To determine drought severity, we use  
390 the Standardised Precipitation-Evapotranspiration Index (SPEI), which is a multi-scalar  
391 drought index that takes into account both precipitation and temperature (see Supplementary  
392 information: Standardised Precipitation-Evapotranspiration drought Index). Total water  
393 storage change (TWSC) derived from NASA's Gravity Recovery and Climate Experiment  
394 (GRACE) observations was used as an integrative measure of water storage change over  
395 continental scale (see Supplementary information: GRACE Terrestrial Total Water Storage  
396 Change). We use gridded rain gauge and temperature datasets provided by the National  
397 Climate Centre, Australian Bureau of Meteorology (see Supplementary information: Gridded  
398 meteorological datasets). Micrometeorological flux tower measured net ecosystem  
399 production (NEP) data (Level 3) is provided by OzFLUX network (see Supplementary  
400 information: In-situ measurements of NEP). To infer the contribution of fire emissions to the  
401 sink-source dynamics and further refine our understanding of carbon loss pathway over  
402 semi-arid ecosystems, we used fire emission data from the fourth-generation global fire  
403 emissions database (GFED4.1s) (see Supplementary information: Global Fire Emissions

404 Database). Major vegetation group map provided by Australian National Vegetation  
405 Information System (NVIS, v4.1) was used to derive the contribution of each biome type to  
406 continental carbon fluxes (see Supplementary information: Vegetation map). The 26 NVIS  
407 vegetation groups were grouped into five major biomes: forest, savanna, shrubland,  
408 grassland, and agriculture. The savanna biome, a tree-shrub-grass multi-strata system,  
409 includes all open forests, woodlands, as well as parts of shrublands, with both *Eucalyptus*,  
410 *Acacia* or other trees as the dominant canopy species. The grassland biome includes  
411 hummock grassland, tussock grassland, and other grassland types.

- 412 1. Keeling, C. D., Chin, J. F. S. & Whorf, T. P. Increased activity of northern vegetation inferred from  
413 atmospheric CO<sub>2</sub> measurements. *Nature* **382**, 146–149 (1996).
- 414 2. Dlugokencky, E. & Tans, P., ESRL Global Monitoring Division – Global Greenhouse Gas Reference  
415 Network. [www.esrl.noaa.gov/gmd/ccgg/trends/](http://www.esrl.noaa.gov/gmd/ccgg/trends/), (2015) (Date of access: 13/09/2016).
- 416 3. Le Quéré, C. et al. The global carbon budget 1959–2011. *Earth Syst Sci Data* **5**, 165–185 (2013).
- 417 4. Raupach, M. R. et al. Global and regional drivers of accelerating CO<sub>2</sub> emissions. *Proc Natl Acad Sci USA*  
418 **104**, 10288–10293 (2007).
- 419 5. Pan, Y. et al. A Large and Persistent Carbon Sink in the World's Forests. *Science*, **333**, 988–993 (2011).
- 420 6. Friedlingstein, P. et al. Climate–carbon cycle feedback analysis: results from the C4MIP model  
421 intercomparison. *J Climate* **19**, 3337–3353 (2006).
- 422 7. Canadell, J. G. et al. Contributions to accelerating atmospheric CO<sub>2</sub> growth from economic activity, carbon  
423 intensity, and efficiency of natural sinks. *Proc Natl Acad Sci USA* **104**, 18866–18870 (2007).
- 424 8. Poulter, B. et al. Contribution of semi-arid ecosystems to interannual variability of the global carbon cycle.  
425 *Nature* **509**, 600–603 (2014).
- 426 9. Ahlström, A et al. The dominant role of semi-arid ecosystems in the trend and variability of the land CO<sub>2</sub>  
427 sink. *Science* **348**, 895–899 (2015).
- 428 10. Keenan, T. F. et al. Terrestrial biosphere model performance for inter-annual variability of land  
429 atmosphere CO<sub>2</sub> exchange. *Glob Change Biol.* **18**, 1971–1987 (2012).
- 430 11. Yi, C. et al. Climate control of terrestrial carbon exchange across biomes and continents. *Environ Res Lett* **5**,  
431 034007 (2010).
- 432 12. Prudhomme, C. et al. Hydrological droughts in the 21st century, hotspots and uncertainties from a global  
433 multimodel ensemble experiment. *Proc Natl Acad Sci USA* **111**, 3262–3267 (2014).
- 434 13. Yi, C., Pendall, E. & Ciais, P. Focus on extreme events and the carbon cycle. *Environ Res Lett* **10**, 070201  
435 (2015).
- 436 14. Rammig, A. & Mahecha, M. D. Ecology: Ecosystem responses to climate extremes. *Nature* **527**, 315–316  
437 (2016).
- 438 15. Ciais, P. et al. Europe-wide reduction in primary productivity caused by the heat and drought in 2003.  
439 *Nature* **437**, 529–533 (2005).
- 440 16. Zeng, N., Qian, H., Rödenbeck, C., Heimann, M. Impact of 1998–2002 midlatitude drought and warming  
441 on terrestrial ecosystem and the global carbon cycle. *Geophys Res Lett* **32**, L22709 (2005).
- 442 17. Zhao, M. & Running, S. W. Drought-induced reduction in global terrestrial Net Primary Production from  
443 2000 through 2009. *Science* **329**, 940–943 (2010).

- 444 18. Reichstein, M. et al. Climate extremes and the carbon cycle. *Nature* **500**, 287–295 (2013).
- 445 19. Anderegg, W. R. L. et al. Pervasive drought legacies in forest ecosystems and their implications for carbon  
446 cycle models. *Science*, **349**, 528–532 (2015).
- 447 20. Forkel, M. et al. Enhanced seasonal CO<sub>2</sub> exchange caused by amplified plant productivity in northern  
448 ecosystems. *Science*, **351**, 696–699 (2016).
- 449 21. Reichstein, M. et al. Reduction of ecosystem productivity and respiration during the European summer 2003  
450 climate anomaly: a joint flux tower, remote sensing and modelling analysis. *Glob Change Biol* **13**, 634–651  
451 (2007).
- 452 22. Schwalm, C. R. et al. Reduction in carbon uptake during turn of the century drought in western North  
453 America. *Nat Geosci* **5**, 551–556 (2012).
- 454 23. Breshears, D. D. et al. Regional vegetation die-off in response to global-change-type drought. *Proc Natl  
455 Acad Sci USA* **102**, 15144–15148 (2005).
- 456 24. Fensham, R. J. et al. Drought-induced tree death in savanna. *Glob Change Biol* **15**, 380–387 (2009).
- 457 25. Huang, K. et al. Tipping point of a conifer forest ecosystem under severe drought. *Environ Res Lett* **10**,  
458 024011 (2015).
- 459 26. Sage, R. F., Christin, P. A. & Edwards, E. J. The C<sub>4</sub> plant lineages of planet Earth. *J Exp Bot* **62**, 3155–3169  
460 (2011).
- 461 27. Morgan, J. A. et al. C<sub>4</sub> grasses prosper as carbon dioxide eliminates desiccation in warmed semi-arid  
462 grassland. *Science* **476**, 202–205 (2011).
- 463 28. Cherwin, K. & Knapp, A. Unexpected patterns of sensitivity to drought in three semi-arid grasslands.  
464 *Oecologia* **169**, 845–852 (2012).
- 465 29. Ponce-Campos, G. E. et al. Ecosystem resilience despite large-scale altered hydroclimatic conditions.  
466 *Nature* **494**, 349–352 (2013).
- 467 30. Moran, M. S. et al. Functional response of U.S. grasslands to the early 21st-century drought. *Ecology* **95**,  
468 2121–2133 (2014).
- 469 31. Ma, X., Huete, A., Moran, M. S., Ponce-Campos, G. & Eamus, D. Abrupt shifts in phenology and  
470 vegetation productivity under climate extremes. *J Geophys Res G* **120**, 2036–2052 (2015).
- 471 32. Scott, R. L., Biederman, J. A., Hamerlynck, E. P., & Barron-Gafford, G. A. The carbon balance pivot point  
472 of southwestern U.S. semiarid ecosystems: Insights from the 21st century drought. *J Geophys Res G* **120**, 2612–  
473 2624 (2015).
- 474 33. Yi, C. et al. Climate extremes and grassland potential productivity. *Environ Res Lett* **7**, 035703 (2012).
- 475 34. Biederman, J. A. et al. Terrestrial carbon balance in a drier world: the effects of water availability in  
476 southwestern North America. *Glob Change Biol* **22**, 1867–1879 (2016).
- 477 35. Yi, C., Wei, S., & Hendrey, G. Warming climate extends dryness-controlled areas of terrestrial carbon  
478 sequestration. *Sci Rep* **4**, 5472 (2014).
- 479 36. Huang, J., Yu, H., Guan, X., Wang, G., & Guo, R. Accelerated dryland expansion under climate change. *Nat  
480 Clim Change* **6**, 166–171 (2016).
- 481 37. Detmers, R. G. et al. Anomalous carbon uptake in Australia as seen by GOSAT. *Geophys Res Lett* **42**,  
482 8177–8184 (2015).
- 483 38. Boening, C. et al. The 2011 La Niña: So strong, the oceans fell. *Geophys Res Lett* **39**, L19602 (2012).
- 484 39. Xie, Z. et al. Spatial partitioning and temporal evolution of Australia's total water storage under extreme  
485 hydroclimatic impacts. *Remote Sens Environ*, **183**, 43–52 (2016).
- 486 40. Haverd, V. et al. The Australian terrestrial carbon budget. *Biogeosci* **10**, 851–869 (2013).
- 487 41. Haverd, V., Smith, B., & Trudinger, C. Dryland vegetation response to wet episode, not inherent shift in  
488 sensitivity to rainfall, behind Australia's role in 2011 global carbon sink anomaly. *Global Change Biol*, **22**,  
489 2315–2316 (2016).
- 490 42. Huang, L. et al. Drought dominates the interannual variability in global terrestrial net primary production by  
491 controlling semi-arid ecosystems, *Sci Rep* **6**, 1–6 (2016).

- 492 43. Cleverly, J. et al. Productivity and evapotranspiration of two contrasting semiarid ecosystems following the  
493 2011 global carbon land sink anomaly. *Agri For Met*, **220**, 151–159 (2016).
- 494 44. Haverd, V., Ahlström, A., Smith, B., & Canadell, J. G. Carbon cycle responses of semi-arid ecosystems to  
495 positive asymmetry in rainfall. *Glob Change Biol* (2016).
- 496 45. Haverd, V., Smith, B., & Trudinger, C. Process contributions of Australian ecosystems to interannual  
497 variations in the carbon cycle. *Environ Res Lett* **11**, 054013 (2016).
- 498 46. Donohue, R. J. et al. Climate-related trends in Australian vegetation cover as inferred from satellite  
499 observations, 1981–2006. *Glob Change Biol* **15**, 1025–1039 (2009).

500

## 501 **Acknowledgements**

502 This work was funded by an Australian Research Council - Discovery Project “*Impact of*  
503 *extreme hydro-meteorological conditions on ecosystem functioning and productivity patterns*  
504 *across Australia*” (ARC-DP140102698, CI Huete). The first author also acknowledges the  
505 support from an Early Career Research Grant (ECRG) from University of Technology  
506 Sydney “*Fingerprinting Australian ecosystem threats from climate change and biodiversity*  
507 *loss*” (PRO16-1358, CI Ma). We would like to thank the opening of flux tower data for public  
508 access by the Australian Terrestrial Ecosystem Research Network (TERN, [www.tern.org.au](http://www.tern.org.au))  
509 – OzFlux facility ([www.ozflux.org.au](http://www.ozflux.org.au)), as well as the availability of multiple processed  
510 satellite products by TERN’s AusCover remote sensing facility ([www.auscover.org.au](http://www.auscover.org.au)). The  
511 ACOS GOSAT data can be obtained from <http://co2.jpl.nasa.gov>. They were produced by the  
512 ACOS/OCO-2 project at the Jet Propulsion Laboratory, California Institute of Technology,  
513 using GOSAT observed spectral radiances made available by the GOSAT project.

## 514 **Author Contributions**

515 X.M. and A.H. conceived the idea and designed the study. X.M. conducted the analyses.  
516 X.M., A.H., J.C., and D.E. drafted the manuscript. F.C., J.C., D.E., J.J., W.M., Z.X.  
517 contributed data to the analysis. B.P., Y.Z., L.G., and G.P.C. contributed to the interpretations  
518 of the results and manuscript writing. All authors contributed to the manuscript revision.

## 519 **Additional information**

520 **Supplementary information** accompanies this paper at <http://www.nature.com/srep>

521 **Competing financial interests:** The authors declare no competing financial interests.